

EXPERIMENTS ON POOL-BOILING HEAT TRANSFER

P. J. BERENSON*

AiResearch Manufacturing Co., Los Angeles 9, California

(Received 22 January 1962)

Abstract—The characteristic pool-boiling curve was measured for *n*-pentane at atmospheric pressure as a function of surface roughness, material and cleanliness. The maximum nucleate-boiling heat flux and the film-boiling curve were independent of surface conditions. The nucleate-boiling heat-transfer coefficient varied by 600 per cent owing to variations in surface finish. It was concluded that transition boiling is a combination of unstable nucleate and unstable film boiling alternating at any location on the heating surface. The transition-boiling heat-transfer data plotted as $\log(q/A)$ vs. $\log(\Delta T)$ was found to be correlated by a straight line connecting the maximum and minimum heat flux points.

I. INTRODUCTION

BOILING heat transfer has received considerable attention during the past decade, the impetus for the increased effort coming from modern developments in technology. The large energy generation rate per unit volume occurring in nuclear reactors and rocket nozzles has required the very high heat-transfer coefficients characteristic of nucleate boiling. The widespread use of various cryogenic fluids has given rise to many situations where large wall superheat temperature differences exist, causing film boiling.

Boiling-heat-transfer data is generally presented graphically with $\log(q/A)$ as the ordinate and $\log(\Delta T)$ as the abscissa where ΔT is the temperature difference between the solid surface temperature and the fluid saturation temperature. The data plotted in this way yields the familiar characteristic boiling curve which has a similar shape for all fluid-surface combinations. The characteristic curve includes three boiling-transfer regimes. In nucleate boiling, which generally occurs over a range of temperature differences from 10 to 100 deg, heat is rapidly transferred from the solid surface to the liquid owing to the stirring action of the bubbles nucleating and growing on the surface. At larger temperature differences, film boiling takes place where the heat is transferred by

conduction through a vapor film which blankets the solid surface. The heat-transfer rate in film boiling is much less than in nucleate boiling. Between the nucleate- and film-boiling regimes lies the transition-boiling region which has the unique characteristic that an increase in temperature difference causes a decrease in heat-transfer rate.

An experimental investigation of pool-boiling heat transfer covering all three boiling regimes is presented below. This investigation was conducted to learn more about the mechanism of heat transfer and the reasons for the transitions from one mode of boiling heat transfer to another. The data lead to conclusions about the mechanism of transition-boiling heat transfer and about the burnout phenomenon.

II. EXPERIMENT DESIGN

The shape of the characteristic boiling curve is such that for a given heat flux three different boiling regimes may be obtained. The transition region is inherently unstable in experiments in which only the heat flux is controlled owing to the negative slope in the transition region. However, an experiment designed to control the temperature difference allows operation within the transition region, as well as the other two regions, since there is only one value of heat flux associated with each value of temperature difference. The most convenient technique for controlling the temperature difference uses a

* Formerly: Assistant Professor of Mechanical Engineering, M.I.T., Cambridge, Massachusetts.

condensing fluid as the heat source. The temperature and pressure of a condensing fluid are dependent; therefore, the temperature can be regulated by controlling the pressure at which condensation occurs, thereby imposing an overall temperature difference. Fig. 1 is a schematic of the test apparatus which is described in detail in [1]. Water, vaporized by electrical heat addition, condensed on the fins on the bottom of the test block A. *n*-Pentane was generally the test fluid with one set of data obtained for carbon tetrachloride. The temperature of the 2 in.-dia. top surface of block A was determined by extrapolating temperatures measured by thermocouples at two axial locations in the block.

This was done both at the center line and near the outer radius of the block to verify that radial temperature gradients were negligible.

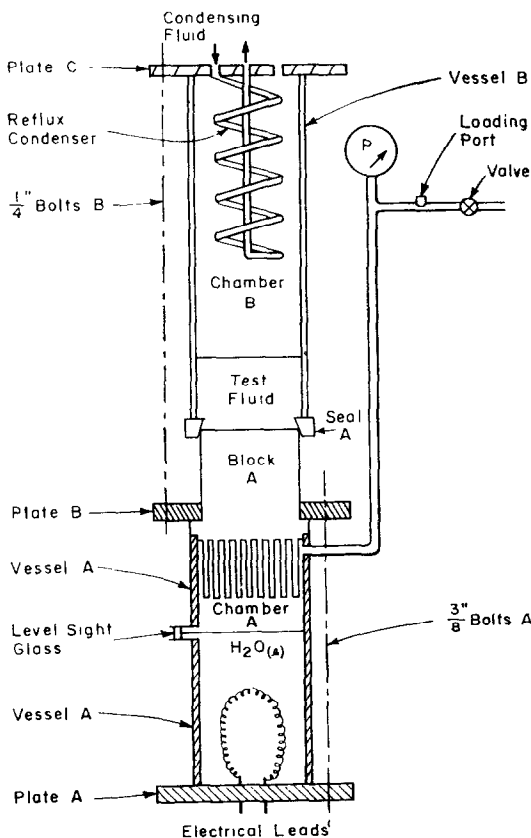


Fig. 1. Test set-up assembly.

The heat flux was determined both by calculating the axial conduction in copper block A and by taking the difference between the electrical energy input and the calibrated heat leak. The two heat-transfer rates agreed within 5 per cent. In the results presented below, the heat flux is calculated by the second method. The saturation temperature of the test fluid in chamber B, established by the existence of atmospheric pressure in chamber B in all tests, was verified by thermocouple measurements.

Chamber B could be dismantled between tests, allowing the surface condition of block A to be varied. The surface roughness was varied by finishing the surface with different grades of lapping compound and emery paper. The details of the surface-roughness finishing techniques are discussed in [1].

To vary the heating surface material a thin disk of the desired material was soldered to the top surface of copper block A. The continuity of the carefully prepared joint was checked visually before and after testing and by measuring the temperature of the copper near the surface at various radial locations.

The test procedure is described in detail in [1]. Enough datum points were measured in each run to define the characteristic boiling curve completely. In particular, great care was taken to define the location of the burnout point and the minimum point. In general, measurements were made as the temperature difference was increased and as it was decreased from point to point, in order to determine the accuracy of the measurements and search for any hysteresis in the boiling curve.

III. DISCUSSION OF RESULTS

A. Results

The most significant runs are presented in Tables 1-12, and graphically, in Figs. 2-7. The uncertainty in the data is different for each boiling regime. The estimated uncertainties are based on measurement-error estimates and the reproducibility of the particular datum point. The uncertainty in the heat flux is presented in the tables for each point. The estimated uncertainty of the temperature difference is small (1-2 deg) and, therefore, uncertainties in heat flux are controlling for most of the datum.

Table 1. *n*-Pentane test data

(Surface material: Ni; surface cleaned with CCl_4 immediately before test. Surface finish: (a) mirror finish, (b) lapped circularly with grit D, no. 160)

(a) Run 38 (5 May 1959)				(b) Run 39 (7 May 1959)			
Point	q/A	Uncertainty	ΔT	Point	q/A	Uncertainty	ΔT
no.	(Btu/h ft ²)	(\pm Btu/h ft ²)	(degF)	no.	(Btu/h ft ²)	(\pm Btu/h ft ²)	(degF)
1	49 000	500	49	1	73 000	800	16
2	68 000	800	64	2	82 000	800	16.5
3	75 000	800	71	3	86 000	800	17
4	77 000	800	75	4	90 000	800	17
5	5800	500	155	5	93 000	800	17.5
6	4800	500	138	6	4800	300	120
7	4500	400	128	7	4700	300	111
8	4200	400	118	8	4500	300	104
9	3800	300	108	9	4700	300	98
10	10 000	300	28	10	5100	300	90
11	17 500	300	35	11	6300	300	68
12	29 000	300	41	12	9500	300	11
13	7900	500	199	13	17 500	300	12
				14	29 000	500	13
				15	45 000	500	14
				16	6800	500	177

Table 2. *n*-Pentane test data

(Surface material: Cu; mirror finish; surface cleaned with CCl_4 immediately before test)

Run 2 (1 November 1958)				Run 3 (4 November 1958)			
Point	q/A	Uncertainty	ΔT	Point	q/A	Uncertainty	ΔT
no.	(Btu/h ft ²)	(\pm Btu/h ft ²)	(degF)	no.	(Btu/h ft ²)	(\pm Btu/h ft ²)	(degF)
1	26 000	500	43	1	7250	200	25
2	40 500	500	52	2	14 500	300	36
3	55 000	500	66	3	24 000	500	44
4	70 000	500	76.5	4	47 000	500	56
5	4200	500	137	5	74 200	500	69
6	3850	500	130	6	78 500	500	73
7	3550	300	120	7	4850	200	142
8	3400	200	110	8	4200	200	124
9	56 500	300	67	9	4000	200	110
10	79 500	400	80	10	7100	300	191
11	82 000	500	85	11	11 000	400	258
12	4200	200	105				
13	5950	200	160				
14	7250	300	181				
15	7730	300	206				

Table 3. *n*-Pentane test data(Surface material: inconel; mirror finish; surface cleaned with CCl_4 immediately before test)

Run 33 (31 March 1959)				Run 36 (16 April 1959)			
Point	q/A	Uncertainty	ΔT	Point	q/A	Uncertainty	ΔT
no.	(Btu/h ft ²)	(\pm Btu/h ft ²)	(degF)	no.	(Btu/h ft ²)	(\pm Btu/h ft ²)	(degF)
1	48 000	800	58	1	41 000	600	54
2	64 000	800	67	2	67 000	800	71
3	71 000	800	76	3	71 000	800	78
4	73 000	800	82	4	5700	500	158
5	5600	500	155	5	4900	500	142
6	4600	400	129	6	4600	400	132
7	4600	400	125	7	4450	400	128
8	5000	400	123	8	4300	400	121
9	53 000	800	61	9	31 000	500	53
10	10 500	300	37	10	10 000	300	39
11	15 500	500	45	11	15 000	500	45
12	23 000	800	49	12	22 000	500	50
13	33 000	800	52	13	51 000	600	63
				14	7200	500	190

Table 4. *n*-Pentane test data(Surface material: inconel; finish: lapped circularly with grit D no. 160; cleaned with CCl_4 immediately before test)

Run 34 (2 April 1959)				Run 35 (4 April 1959)			
Point	q/A	Uncertainty	ΔT	Point	q/A	Uncertainty	ΔT
no.	(Btu/h ft ²)	(\pm Btu/h ft ²)	(degF)	no.	(Btu/h ft ²)	(\pm Btu/h ft ²)	(degF)
1	71 000	800	28	1	71 000	800	27
2	79 000	800	30	2	79 500	800	30
3	4700	300	111	3	5000	500	122
4	5800	300	98	4	5000	400	108
5	7500	500	92	5	6400	500	95
6	9500	600	86	6	10 000	600	82
7	54 000	600	25	7	45 000	600	23
8	11 000	300	17	8	14 500	300	18
9	20 000	500	19	9	27 000	500	20
10	35 000	500	22	10	6700	500	165
				11	9100	600	220

Table 5. *n*-Pentane test data

(Surface material: Cu; finish: lapped in one direction with grit E no. 120; cleanliness: slightly oxidized, not cleaned before test)

Run 7 (15 November 1958)			
Point	q/A	Uncertainty	ΔT
no.	(Btu/h ft ²)	(\pm Btu/h ft ²)	(degF)
1	93 500	1000	45
2	6600	300	13
3	25 300	300	15
4	44 000	600	17
5	74 000	800	21
6	92 500	1000	25
7	99 000	1000	30
8	75 000	1000	72
9	40 000	800	121
10	18 000	600	157
11	9800	500	187
12	9000	500	209
13	15 000	500	171
14	27 200	600	142
15	9650	500	234
16	12 000	600	267

Table 6. *n*-Pentane test data

(Surface material: Cu; finish: lapped in one direction with grit E no. 120; cleaned with CCl₄ immediately before test)

Run 10 (28 November 1958)			
Point	q/A	Uncertainty	ΔT
no.	(Btu/h ft ²)	(\pm Btu/h ft ²)	(degF)
1	4300	300	110
2	4200	300	91
3	4500	300	75
4	9300	500	60
5	13 000	500	50
6	20 500	800	41
7	60 000	800	17
8	6600	300	11
9	21 000	300	13
10	44 000	800	15
11	7900	500	65
12	89 500	1000	19
13	6600	300	70
14	3850	300	81
15	4000	400	104
16	4650	500	138
17	6600	500	178
18	8500	500	221
19	11 000	600	263

Table 7. *n*-Pentane test data

(Surface material: Cu; finish: lapped in one direction with grit E no. 120; cleanliness: oxidized, not cleaned before test)

Run 8 (20 November 1958)				Run 9 (22 November 1958)			
Point	q/A	Uncertainty	ΔT	Point	q/A	Uncertainty	ΔT
no.	(Btu/h ft ²)	(\pm Btu/h ft ²)	(degF)	no.	(Btu/h ft ²)	(\pm Btu/h ft ²)	(degF)
1	90 000	1000	52	1	95 000	1000	46
2	13 800	300	14	2	64 500	1000	102
3	33 000	800	16	3	9500	300	14
4	59 000	800	19	4	19 000	300	15
5	85 000	800	23	5	47 000	600	18
6	100 000	1000	28	6	76 500	800	22
7	97 000	1000	41	7	103 000	1000	34
8	75 000	1000	84	8	83 000	1000	72
9	10 300	500	167	9	43 500	1000	123
10	28 000	600	141	10	23 500	800	143
11	21 500	600	153	11	9500	800	177
12	9800	500	187	12	16 500	800	157
13	9700	500	221	13	9200	500	194
14	12 000	600	266	14	9500	500	230
				15	10 800	600	260

Table 8. *n*-Pentane test data(Surface material: Cu; finish: lapped circularly with grit E no. 120; cleaned with CCl₄ immediately before test)

Run 16 (27 December 1958)				Run 17 (30 December 1958)			
Point	q/A	Uncertainty	ΔT	Point	q/A	Uncertainty	ΔT
no.	(Btu/h ft ²)	(\pm Btu/h ft ²)	(degF)	no.	(Btu/h ft ²)	(\pm Btu/h ft ²)	(degF)
1	55 000	800	13	1	6700	300	109
2	7400	200	9	2	6400	300	81
3	28 500	300	11	3	10 500	300	60
4	82 000	800	14	4	16 700	800	43
5	92 000	1000	16	5	62 000	800	13
				6	20 600	400	10
				7	90 000	800	14
				8	5800	300	91
				9	7700	300	70
				10	5500	400	104
				11	6450	400	138
				12	7250	500	180
				13	9350	500	226

Table 9. Carbon tetrachloride test data

(Surface material: Cu; finish: lapped circularly with grit E no. 120; cleaned with CCl₄ immediately before test)

Run 19 (31 January 1959)				Run 20 (2 February 1959)			
Point	q/A	Uncertainty	ΔT	Point	q/A	Uncertainty	ΔT
no.	(Btu/h ft ²)	(\pm Btu/h ft ²)	(degF)	no.	(Btu/h ft ²)	(\pm Btu/h ft ²)	(degF)
1	37 000	800	17	1	13 000	500	15
2	72 000	800	20	2	45 000	600	18
3	91 000	800	22	3	90 000	800	23
4	6500	400	96	4	99 000	800	24
5	3500	400	138	5	7700	500	99
6	9700	400	84	6	5000	500	121
7	14 500	300	68	7	4500	500	143
8	23 000	800	53	8	5500	600	170
9	7300	300	15	9	6750	700	193
10	94 500	800	23				
11	98 500	800	25				
12	4800	500	168				
13	6300	600	197				

Table 10 *n*-Pentane test data

(Surface material: Cu; finish: lapped circularly with grit E no. 120; cleaned with CCl_4 immediately before test: (a) surface oxidized, (b) photographs taken for bubble diameter measurements)

(a) Run 22 (7 February 1959)				(b) Run 23 (10 February 1959)			
Point	q/A	Uncertainty	ΔT	Point	q/A	Uncertainty	ΔT
no.	(Btu/h ft ²)	(\pm Btu/h ft ²)	(degF)	no.	(Btu/h ft ²)	(\pm Btu/h ft ²)	(degF)
1	5500	300	110	1	11 500	300	55
2	5800	300	76	2	19 000	800	40
3	15 000	600	46	3	94 500	800	16
4	10 500	300	9	4	6600	400	93
5	33 500	300	11	5	11,500	600	261
6	88 500	800	14				
7	96 000	800	16				
8	6000	300	93				
9	6600	400	147				
10	8000	500	193				

Table 11. *n*-Pentane test data

(Surface material: Cu; cleaned with CCl_4 immediately before test; finish: (a) no. 320, (b) no. 60 emery rubbed in one direction)

(a) Run 31 (17 March 1959)				(b) Run 32 (19 March 1960)			
Point	q/A	Uncertainty	ΔT	Point	q/A	Uncertainty	ΔT
no.	(Btu/h ft ²)	(\pm Btu/h ft ²)	(degF)	no.	(Btu/h ft ²)	(\pm Btu/h ft ²)	(degF)
1	71 000	800	35	1	79 000	800	23
2	86 000	800	38	2	91 000	1000	26
3	90 000	800	42	3	96 000	1000	27
4	4000	300	121	4	100 000	1000	29
5	3700	300	99	5	4000	400	121
6	4600	500	88	6	3400	300	102
7	7700	600	82	7	3800	300	87
8	13 500	800	23	8	6900	500	79
9	26 500	300	27	9	16 000	300	14
10	49 000	800	31	10	29 000	300	16
11	3000	300	110	11	52 000	800	19
12	5100	400	154	12	4500	400	149
13	6700	400	193	13	7700	500	213
14	9600	500	245				

Table 12. *n*-Pentane test data

(Surface material: Cu; finish: lapped circularly with grit E no. 120; cleaned with CCl_4 immediately before test)

Run 25 (17 February 1959)			
Point no.	q/A (Btu/h ft ²)	Uncertainty (\pm Btu/h ft ²)	ΔT (degF)
1	6100	400	109
2	6800	400	75
<i>three drops of oleic acid added</i>			
3	54 000	1000	72
4	34 000	800	41
5	22 000	300	10
6	86 000	800	15
7	93 000	800	16
8	42 000	800	54
<i>three drops of oleic acid added</i>			
9	78 000	1000	52

B. Nucleate boiling

Fig. 2 shows the large effect of surface roughness on the temperature difference required to transfer a given heat flux in nucleate boiling. These results strongly emphasize the importance of including the surface roughness in any theoretical analysis of nucleate-boiling heat transfer. The results presented in Fig. 2 indicate that r.m.s. roughness is not the significant roughness parameter. Although the r.m.s. roughness of the various surfaces was not measured, it was obvious that the r.m.s. roughness of the emery-finished surfaces was greater than that of either the lapped surface or the "mirror" finished surface. Westwater *et al.* [2] determined visually that in general bubbles nucleate from cavities on the heating surface, and therefore the "rougher" surface with regard to boiling is that which has the greater number of cavities of appropriate size, regardless of the r.m.s. roughness. For example, lapping is generally thought of as producing a smooth finish, and this is true in the conventional mechanical sense. However, a lapping compound contains small pieces of grit suspended in oil which, when rubbed on a solid surface, essentially saturate the surface with small cavities. This condition, while

corresponding to a small r.m.s. roughness, is ideal for bubble nucleation as shown in Fig. 2.

Figs. 3 and 4 present the results obtained for the two extremes of roughness when inconel and nickel were used as the heating surface. Once again the large effect of roughness on nucleate boiling is shown. In addition, the temperature difference required to produce a given heat flux for the same surface-finishing technique depends on the surface material. Some of this dependency may be due to differences in the hardness which would tend to change the cavity size and density distribution on the surface. However, the behavior of the data indicates that the surface thermal properties do affect nucleate boiling. Any thermal resistance associated with the transient conduction process occurring near a bubble nucleation site would tend to become more significant as the thermal resistance of the surface material increased or as the thermal resistance of the boiling-fluid boundary decreased. This is consistent with the observed increase in ΔT as thermal conductivity (diffusivity) decreases and the fact that the effect is largest for roughness having the highest heat-transfer coefficient.

C. Film boiling

The solid line in the film-boiling regions of all figures is identical. It can be seen that none of the surface properties, i.e. roughness and material, affect the film-boiling data. This was to be expected since, in film boiling, heat is transferred by conduction through a vapor film and, unless the surface roughness were great enough to disturb the vapor film, the conduction process would not be influenced by surface characteristics.

D. Transition boiling

1. *Introduction.* It was found, with the exception of some of the data presented in Fig. 5, that the transition-boiling data lie along a straight line connecting the burnout point and the film-boiling minimum point on log-log graph paper. This is also true of the transition boiling data obtained by Braunlich [3] and Kaulakis and Sherman [4]. Since the location of the burnout point depends upon surface conditions, as can be seen from Figs. 2-4. The fact that

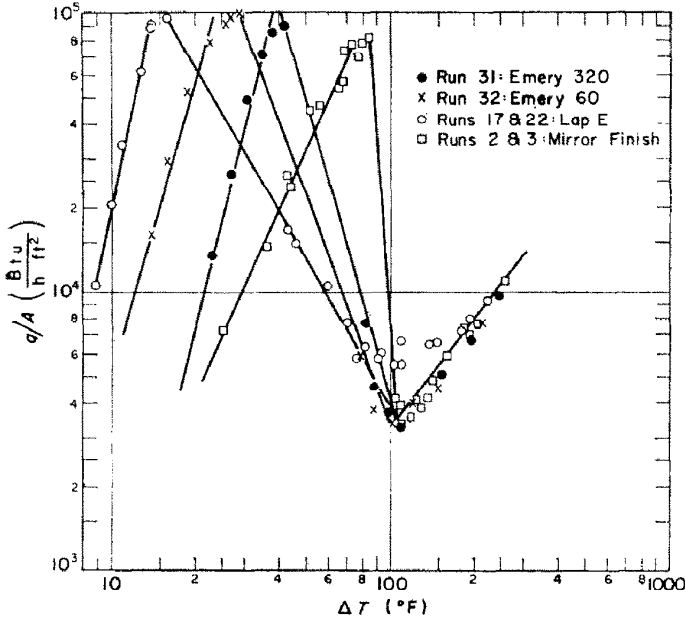


Fig. 2. Copper-pentane test results: effect of roughness.

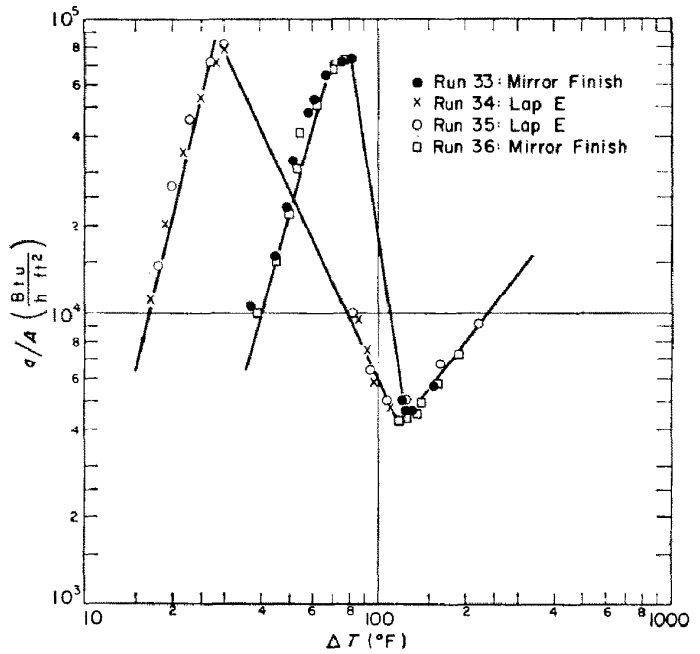


Fig. 3. Inconel-pentane test results: effect of roughness.

FIG. 4. Nickel-pentane test results: effect of roughness.

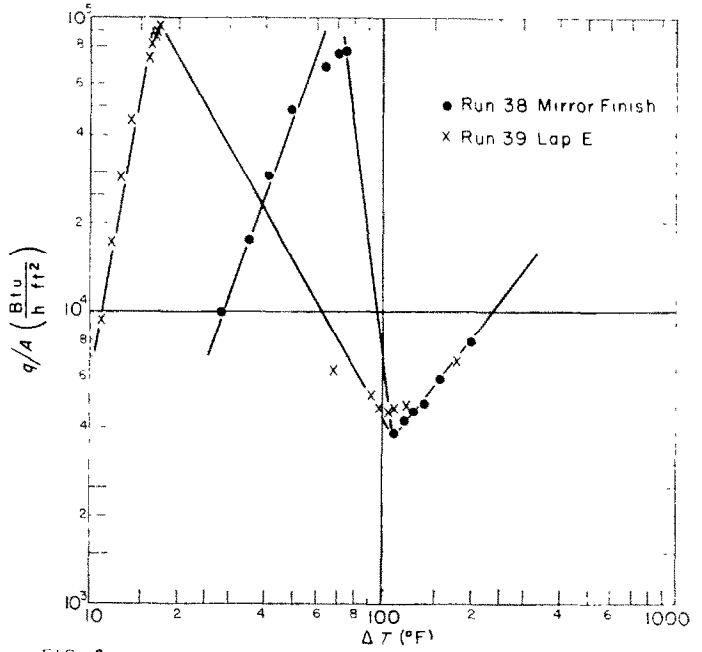


FIG. 4

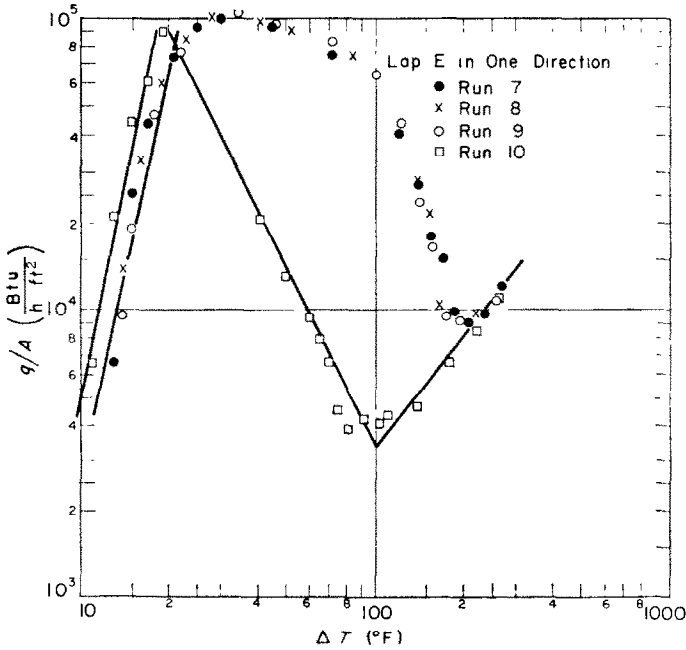


FIG. 5. Copper-pentane test results: effect of surface cleanliness.

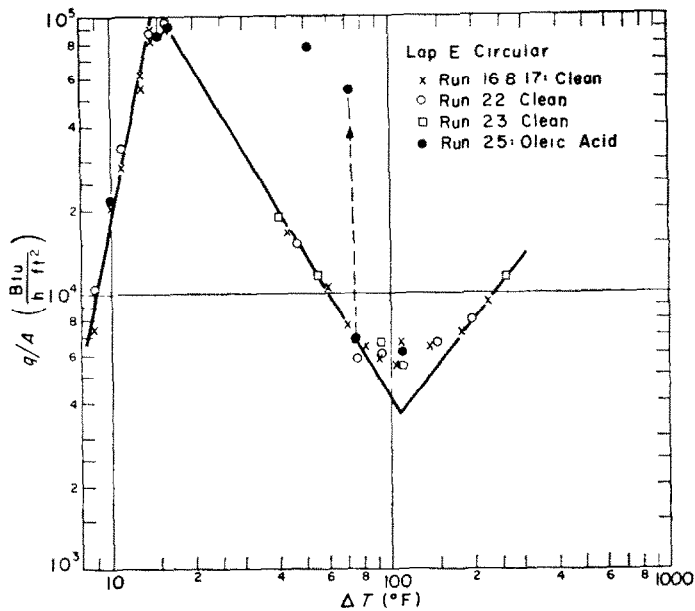
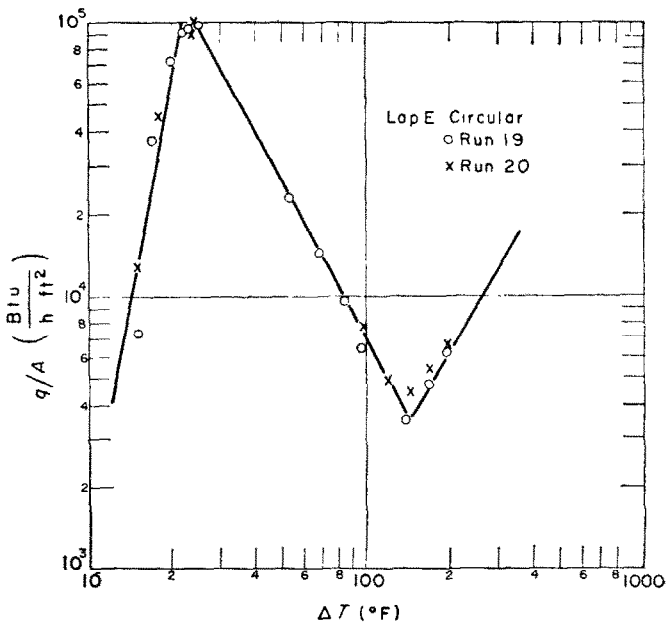


FIG. 6. Copper-pentane test results: effect of wetting agent.

FIG. 7. Copper-carbon tetrachloride test results.



surface roughness is unimportant in film boiling, but has a significant effect on transition boiling, implies that a continuous vapor film does not cover the surface in the transition region.

The following discussion of the experiments demonstrating that surface energy (contact angle) affects transition boiling shows that liquid–solid contact exists in this regime. This fact and the theoretical explanations for the maximum and minimum heat flux are combined to yield a description of the mechanism of transition-boiling heat transfer.

2. *Effect of surface cleanliness.* Figures 5 and 6 present data substantiating the tentative conclusion that liquid–solid contact occurs in transition boiling. The difference between run 10 and the other runs in Fig. 5 is that, immediately prior to run 10, the copper surface was freshly lapped and cleaned with a paper towel saturated with carbon tetrachloride, while in the other runs the surface which had oxidized owing to exposure to the atmosphere between runs was not cleaned with carbon tetrachloride. Therefore, any dirt particles in the air which deposited on the surface would contaminate the surface during the test run. It was determined in run 22, Fig. 6, that an oxidized, cleaned surface had the same boiling characteristics as an unoxidized, cleaned surface. Therefore, it was concluded that atmospheric dirt depositing on the surface between tests where it would tend to change surface energy (contact angle) conditions was the cause of the large effect shown in Fig. 5. To verify this conclusion run 25, shown in Fig. 6, was performed in which the surface material, roughness, and cleaning procedure were identical to runs 17, 22 and 23. Once the complete boiling curve had been defined as indicated by the solid circles in Fig. 6, a drop of a known surface-active agent, oleic acid, was added to the boiling fluid. The result was a complete change in the boiling process from the quiet mode characteristic of low-heat-flux film boiling to the chaos characteristic of the burnout point. In particular, the heat flux increased by an order of magnitude. It was not possible to obtain the complete boiling curve under these conditions since the oleic acid apparently gradually disappears from the surface so that the heat flux at a given temperature

difference decreases with time toward the “clean” value. However, two datum points were measured immediately after addition of the oleic acid, thus defining the general location of the boiling curve in the transition region. The magnitude of the effect on the transition region is the same in Fig. 6 as observed in Fig. 5, confirming that surface contamination caused the change.

To further verify the above conclusion, both the liquid–vapor surface tension and the contact angle were measured. The liquid–vapor surface tension was measured with the capillary height method described by Harkins [5]. The absolute value of the surface tension measured was equal to the value given in the literature [6] within the ± 5 per cent accuracy of the measurement. No observable change of *n*-pentane surface tension occurred due to the addition of oleic acid as should be the case for these fluids according to Harkins [5].

The contact angle was measured from an elevation photograph of a drop of liquid *n*-pentane placed on a horizontal surface. The estimated accuracy of the measurement and the reproducibility was $\pm 1^\circ$. For pure *n*-pentane on copper cleaned with carbon tetrachloride the measured contact angle was 10° . The addition of a slight amount of oleic acid to the *n*-pentane resulted in spreading (i.e. no contact angle). Spreading also occurred for pure *n*-pentane placed on copper left exposed to the atmosphere, confirming the conclusion that the change in the transition-boiling data was due to a change in contact angle (surface energy).

These results lead to the conclusion that the liquid touches the solid surface in transition boiling. Contact angle and spreading phenomena occur only if a triple interface is present. If changing the value of these quantities affects the data, then a triple interface must exist. This could occur only if liquid–solid contact existed, as well as vapor–solid contact. Therefore, since varying the contact angle caused a change in the transition boiling curve, liquid–solid contact must occur in the transition region.

3. *Mechanism of transition boiling.* Zuber [7] has shown that the maximum heat flux of transition boiling, which is also the maximum heat flux of nucleate boiling, is a result of a Helmholtz

Instability. That is, the vapor generated by the maximum heat flux corresponds to the maximum counterflow of vapor and liquid normal to the heating surface which can occur in steady flow and remain stable.

The minimum heat flux of transition boiling which is also the minimum heat flux of film boiling is a result of Taylor Instability [7]. The vapor generated by heat transfer through the vapor film, below a certain temperature difference, is not great enough to supply the vapor demanded by the growth and bubble departure rates of the liquid-vapor boundary which are determined by Taylor Hydrodynamic Instability.

At temperature differences within the transition region, the amount of vapor generated by film boiling is too small to support the vapor film and the amount of vapor generated by nucleate boiling is too great to allow sufficient liquid to reach the heating surface in steady flow. Therefore, the writer concludes that each of these boiling-heat-transfer mechanisms occur alternately at a given location on the heating surface. Heat is transferred through a vapor film at a rate which is not great enough to generate the vapor mass flow necessary to support the film; therefore the film collapses. Heat is next transferred directly to the liquid, which contacts the surface when the vapor film collapses, generating vapor at such a high rate that the liquid necessary to sustain the heat-transfer-vapor-generation rate is unable to reach the surface. Therefore, a vapor blanket once again forms.

As the temperature difference approaches the value at the minimum heat flux, film boiling becomes more stable and nucleate boiling becomes more unstable, where the relative stability is determined by the amount of time it takes for the given mode of heat transfer to collapse. That is, the amount of vapor generated by heat conduction through the vapor film becomes almost great enough to support the film, and the amount of vapor generated by nucleate boiling is much greater than the maximum steady-state value allowed by Helmholtz Hydrodynamic Instability, resulting in a rapid collapse of the nucleate mode of boiling. Therefore, as the temperature difference approaches the value at the minimum, the fraction of time during which

film boiling exists increases until, at the minimum, film boiling is stable and exists steadily. The reverse reasoning applies when approaching the temperature difference at the maximum. That is, nucleate boiling becomes more stable and film boiling less stable.

In summary, the author concludes that transition boiling is a combination of unstable film boiling and unstable nucleate boiling, each of which alternately exists at a given location on the heating surface. The variation of average heat-transfer rate with temperature difference is concluded to be primarily a result of the change in the fraction of time with which each boiling regime exists at a given location.

E. *Minimum film-boiling heat flux*

The value of the minimum heat flux for a clean surface might be called the minimum-minimum, since with a wetting agent added the minimum occurs at a higher heat flux, although still along the same film-boiling curve. The minimum-minimum is independent of surface material and can be predicted analytically [1]. It is of interest to determine the dividing line between clean and dirty surfaces in regard to the location of the minimum; if surfaces are in general clean, the minimum-minimum occurs. As a result of the contact-angle measurements, it is found that the minimum-minimum exists for contact angles as low as 10° , at least for *n*-pentane. In general, engineering surfaces have a contact angle of approximately 50° [8, 10]. Therefore, it appears that the minimum-minimum generally occurs in practice.

It is plausible to suggest that the minimum-minimum will occur as long as any finite value of the contact angle exists, i.e. as long as spreading does not occur. It is difficult to conceive of how a change of a few degrees in the contact angle could cause the large effects shown in Figs. 5 and 6. However, there is considerable difference between the condition where a drop statically sits on a surface and that where it spreads over the surface. Borishansky [9] has shown that the liquid instantaneously contacts the solid surface in film boiling after a bubble breaks away from the two-phase interface. If the liquid spreads sufficiently fast upon contacting the surface a vapor film may not reform.

Therefore, under these conditions the location of the minimum would depend upon spreading rate.

The fact that the liquid contacts the surface instantaneously in film boiling also explains why no hysteresis is observed at the minimum. The value of the minimum heat flux for dirty surfaces depends upon the rate of spreading. However, since the liquid contacts the surface every time a bubble departs in film boiling, whenever the conditions are appropriate to allow the liquid to remain in contact with the surface, it will occur with no hysteresis, even when decreasing the temperature difference in the film-boiling regime.

F. Maximum nucleate-boiling (burnout) heat flux

Zuber [7] predicted the maximum heat flux on the assumption that it is due to the Helmholtz Instability of the counterflowing vapor and liquid near the heating surface. If this is true, the value of the maximum heat flux is independent of surface conditions since the limiting condition is a hydrodynamic phenomenon. The experimental results show that this is the case. In particular, referring to Fig. 2, it is seen that while the temperature difference at the maximum point varies by 500 or 600 per cent, the value of the burnout heat flux essentially remains constant. There is a reproducible variation of approximately 10 per cent, which for engineering purposes may be neglected.

Data has been presented in the literature which presumably indicates that the burnout heat flux can be made to vary by changes in surface conditions. However, in all of the tests with which the writer is familiar the measured burnout heat flux was less than that predicted by the Zuber correlation. This can be explained as follows. Boiling is a local phenomenon while in heat-transfer experiments the average heat flux is measured. Therefore, if different sections of the heating surface have different nucleate-boiling curves the measured results will be an average of the various curves. This would occur if the roughness was not uniform, if the gravity varied, e.g. around the periphery of horizontal tubes, etc. Since the average must always be less than the highest local heat flux existing at a given temperature difference, the maximum

heat flux measured will always be less than the maximum occurring locally.

An explanation can also be offered for the apparent increase in the burnout heat flux which has been observed as a result of adding trace additives to boiling fluids. If the heating surface is such that the measured average burnout heat flux is less than the local burnout heat flux, e.g. horizontal tube, the addition of a wetting agent which causes spreading will tend to broaden the burnout point, as shown in Figs. 5 and 6. Therefore, since the maximum heat flux exists over a large range of temperature difference, the maximum measured for the surface will equal the maximum predicted, even though this maximum will initially be attained at different ΔT 's for different sections of the surface. In summary, in order to be confident of attaining the maximum heat flux predicted by the Zuber correlation, uniform surface conditions must exist.

IV. SUMMARY OF RESULTS AND CONCLUSIONS

(A) The nucleate-boiling heat-transfer coefficient can be changed by 500–600 per cent owing to changes in surface roughness.

(B) The film-boiling portion of the boiling curve is independent of surface material, cleanliness and roughness, provided that the roughness height is less than the film thickness.

(C) All of the variables which affect the nucleate-boiling heat-transfer rate affect the transition-boiling heat-transfer rate in the same way.

(D) Since contact angle proves to be an important variable in transition boiling, liquid-solid contact as well as vapor-solid contact must occur in transition boiling.

(E) For contact angles of commercial importance, the location of the film-boiling minimum point is independent of the surface material and roughness. The minimum heat flux obtained in these circumstances is the hydrodynamically limited minimum heat flux. Higher values of minimum heat flux prevail when spreading takes place.

(F) The relation between heat flux and temperature difference in the transition region is generally correlated by a straight line connecting

the burnout point with the minimum-minimum point on log-log graph paper.

(G) Transition boiling is a combination of unstable film boiling and unstable nucleate boiling alternately existing at any given location on the heating surface. The variation of heat-transfer rate with temperature difference is primarily a result of a change in the fraction of time each boiling regime exists at a given location.

(H) The maximum nucleate-boiling burnout heat flux is essentially independent of surface material, roughness and cleanliness.

ACKNOWLEDGEMENTS

Professor Peter Griffith of M.I.T. was a constant source of guidance, technical assistance and encouragement. The research was supported by the National Science Foundation through NSF Grant No. G-6305.

REFERENCES

1. P. J. BERENSON, *On Transition Boiling Heat Transfer from a Horizontal Surface*. Thesis, M.I.T., Cambridge, Mass. (1960).
2. H. B. CLARK, P. S. STRENGE and J. W. WESTWATER, Active sites for nucleate boiling. *A.I.Ch.E.-A.S.M.E. Second Nat. Heat Transfer Congress*, Prepr. no. 13, Chicago (1958).
3. R. H. BRAUNLICH, *Heat Transfer to Boiling Liquids Vacuum*. Thesis, M.I.T., Cambridge, Mass. (1941).
4. E. G. KAULAKIS and L. M. SHERMAN, Thesis, M.I.T., Cambridge, Mass. (1938).
5. W. D. HARKINS, *Physical Chemistry of Surface Films* pp. 64, 284. Reinhold, New York (1954).
6. M. T. CICHELLI and C. F. BONILLA, Heat transfer to liquids boiling under pressure. *Trans. Amer. Inst. Chem. Engrs* 41, 755 (1945).
7. N. ZUBER, *Hydrodynamic Aspects of Boiling Heat Transfer*. Thesis, U.C.L.A. (1959).
8. P. GRIFFITH and J. D. WALLIS, Role of surface conditions in nucleate boiling. *A.S.M.E.-A.I.Ch.E. Third Nat. Heat Transfer Conference*, Prepr. no. 106, Storrs, Conn. (1959).
9. V. M. BORISHANSKY, Heat transfer to a liquid freely flowing over a surface heated to a temperature above the boiling point, in *Problems of Heat Transfer During a change of State* (Ed. by S. S. KUTATELADZE) AEC-tr-3405 (1953).
10. C. CORTY and A. S. FOUST, Surface variables in nucleate boiling. *A.I.Ch.E. Heat Transfer Symposium*, Prepr. no. 1, St. Louis, Mo. (1953).

Résumé—La courbe d'ébullition caractéristique a été tracée pour le *n*-pentane à la pression atmosphérique en fonction de la rugosité de surface, du matériau et de sa propreté. Le flux de chaleur maximum dû à l'ébullition nucléée et la courbe d'ébullition par film sont indépendants des conditions de surface. Le coefficient de transmission de chaleur par ébullition nucléée peut varier de 600% suivant l'état de la surface. On en conclut que l'ébullition transitoire est une combinaison de l'ébullition instable nucléée et de l'ébullition instable par film qui alterne en des points quelconques de la surface chauffante. Les données en $\log(q/A)$ en fonction de $\log(\Delta T)$ sont représentées par une droite qui relie les points du flux de chaleur maximum à ceux du flux de chaleur minimum.

Zusammenfassung—In Abhängigkeit von Oberflächenrauigkeit, Material und Reinheit wurde die charakteristische Siedekurve bei freier Konvektion für *n*-Pentan unter Atmosphärendruck ermittelt. Der maximale Wärmefluss beim Blasensieden und die Kurve des Filmsiedens zeigten sich von den Oberflächenbedingungen unabhängig. Beim Blasensieden änderte sich der Wärmeübergangskoeffizient je nach Oberflächenbeschaffenheit bis zu 600%. Übergangssieden wird als Kombination von instabilem Blasensieden und instabilem Filmsieden mit wechselnder Verteilung über die Heizfläche betrachtet. Die Wärmeübergangsdaten für Übergangssieden sind als $\log(q/A)$ zu $\log(\Delta T)$ gezeichnet und liessen sich durch eine gerade Verbindungslinie der Punkte maximalen und minimalen Wärmeflusses korrelieren.

Аннотация—Построена характеристическая кривая кипения нормального пентана при атмосферном давлении в зависимости от шерховатости поверхности, свойств материала и его чистоты. Максимальный тепловой поток при пузырьковом кипении и тепловой поток при пленочном кипении не зависят от условий на поверхности. Коэффициент теплообмена при пузырьковом кипении изменялся на 600%, что было вызвано различной обработкой поверхности. Установлено, что переходный режим кипения представляет собой чередующиеся в любой точке поверхности нагрета неустановившееся ядерное и неустановившееся пленочное кипение. По экспериментальным данным построен график зависимости $\log(g/A)$ от $\log(\Delta T)$ в процессе теплообмена при кипении. График представляет собой прямую, проведенную через точки максимального и минимального тепловых потоков.